nature plants

ARTICLES

PUBLISHED: 9 MAY 2016 | ARTICLE NUMBER: 16050 | DOI: 10.1038/NPLANTS.2016.50

Role of bifunctional ammonia-lyase in grass cell wall biosynthesis

Jaime Barros[1,2], Juan C. Serrani-Yarce[1,2], Fang Chen[1,2,3], David Baxter[1], Barney J. Venables[1] and Richard A. Dixon[1,2,3]*

L-Phenylalanine ammonia-lyase (PAL) is the first enzyme in the biosynthesis of phenylpropanoid-derived plant compounds such as flavonoids, coumarins and the cell wall polymer lignin. The cell walls of grasses possess higher proportions of syringyl (S)-rich lignins and high levels of esterified coumaric acid compared with those of dicotyledonous plants, and PAL from grasses can also possess tyrosine ammonia-lyase (TAL) activity, the reason for which has remained unclear. Using phylogenetic, transcriptomic and *in vitro* biochemical analyses, we identified a single homotetrameric bifunctional ammonia-lyase (PTAL) among eight BdPAL enzymes in the model grass species *Brachypodium distachyon*. ^{13}C isotope labelling experiments along with *BdPTAL1*-downregulation in transgenic plants showed that the TAL activity of BdPTAL1 can provide nearly half of the total lignin deposited in *Brachypodium*, with a preference for S-lignin and wall-bound coumarate biosynthesis, indicating that PTAL function is linked to the characteristic features of grass cell walls. Furthermore, isotope dilution experiments suggest that the pathways to lignin from L-phenylalanine and L-tyrosine are distinct beyond the formation of 4-coumarate, supporting the organization of lignin synthesis enzymes in one or more metabolons.

Land colonization by plants in the Devonian was a key step towards the development of terrestrial ecosystems. Ancestral land plants had to face stresses such as ultraviolet irradiation, desiccation and attack by soil microbial communities, which drove key adaptations, including the emergence of specialized metabolic pathways[1,2]. L-Phenylalanine (L-Phe) and L-tyrosine (L-Tyr) are aromatic amino acids used for the synthesis of proteins, and in plants they also serve as precursors of numerous natural products with diverse biological functions such as signal molecules, cell wall structural components, phytoalexins, pigments and ultraviolet protectants[3]. Both these aromatic amino acids are derived from the shikimate pathway, to which more than 30% of photosynthetically fixed carbon is directed in vascular plants toward the synthesis of the lignin biopolymer via the phenylpropanopid pathway[4].

The first step in the phenylpropanoid pathway is the deamination of L-Phe into *trans*-cinnamic acid by PAL; subsequently, 4-coumaric acid (4CA) is synthesized via the *para*-hydroxylation of the aromatic ring by cinnamate-4-hydroxylase (C4H). Alternatively, 4CA can also be formed directly from L-Tyr by TAL (Supplementary Fig. 1). Caffeic acid is derived by further hydroxylation of 4CA on the C3 position of the aromatic ring, a reaction now considered to take place primarily at the level of the coumaroyl shikimate/quinate ester[5]. The hydroxyl group of the caffeate moiety, either as a free acid or a coenzyme A (CoA) ester, can be methylated to yield ferulic acid or feruloyl-CoA, respectively (Supplementary Fig. 1).

In general, ammonia-lyases are specific for their individual substrates[6–8]. However, PTALs, common among monocots but also found in some dicots and fungi, have the ability to deaminate both L-Phe and L-Tyr with similar efficiency[9–12]. Although both PAL and TAL activities found in PTALs are known to reside in the same polypeptide[10], the enzyme kinetics and subunit structures of PTALs have not been fully studied. Moreover, the in planta role of PTAL has been debated for many years with no firm conclusions[13,14]. PTAL-derived TAL activity in grasses provides an alternative route to 4CA that bypasses the hydroxylation of cinnamic acid by the membrane-bound cytochrome-P450 monooxygenase C4H (Supplementary Fig. 1), but whether this is in any way related to the composition of grass cell walls, with their high levels of syringyl lignin units and esterified coumaric acid, remains unclear.

Results

By using a comparative genomic approach we identified one candidate in the *Brachypodium* genome (BdPTAL1 XP_003575396) that is homologous to previously reported genes encoding PTAL proteins (*Zea mays* NP_001105334, *Panicum virgatum* Pavirv00064275m and *Bambusa oldhamii* ADE00261) (Fig. 1a). Phylogenetic analysis revealed that BdPTAL1 fell within a monocot clade containing previously characterized PTALs, most of them having the His residue (His 89 of *Rhodobacter sphaeroides* (Rs)TAL) considered determinant for substrate selectivity to include L-Tyr[15,16] (Supplementary Fig. 2). *BdPTAL1* is closely related to seven other *Brachypodium* genes that appear, on the basis of amino acid sequence, to encode mono-functional *PALs* (Supplementary Table 1 and Supplementary Fig. 2)[17,18]. Based on peptide sequence similarity, no other genes were found in the *Brachypodium* genome that could encode putative ammonia-lyases. To find homologous *PTAL* genes in available grass genomes, we used the BdPTAL1 protein sequence to search the NCBI protein database using the Basic Local Alignment Search Tool (BLAST) with default parameters (protein-protein BLAST Expect (E) value $\leq 10^{-5}$). All proteins with a percentage identity higher than 75% were selected and studied further. Comparative analysis showed that rice, corn and sugarcane have six *BdPTAL1* orthologs, foxtail millet five, wheat and sorghum three, bamboo and switchgrass two, and oat, barley and *Brachypodium* just one (Supplementary Fig. 3). Therefore, *B. distachyon* is an excellent candidate for studies on PTAL function.

[1]BioDiscovery Institute, University of North Texas, Denton, Texas 76203, USA. [2]Department of Biological Sciences, University of North Texas, Denton, Texas 76203, USA. [3]BioEnergy Science Center (BESC), Oak Ridge National Laboratory, Oak Ridge, Tennessee 37831, USA. *e-mail: Richard.Dixon@unt.edu

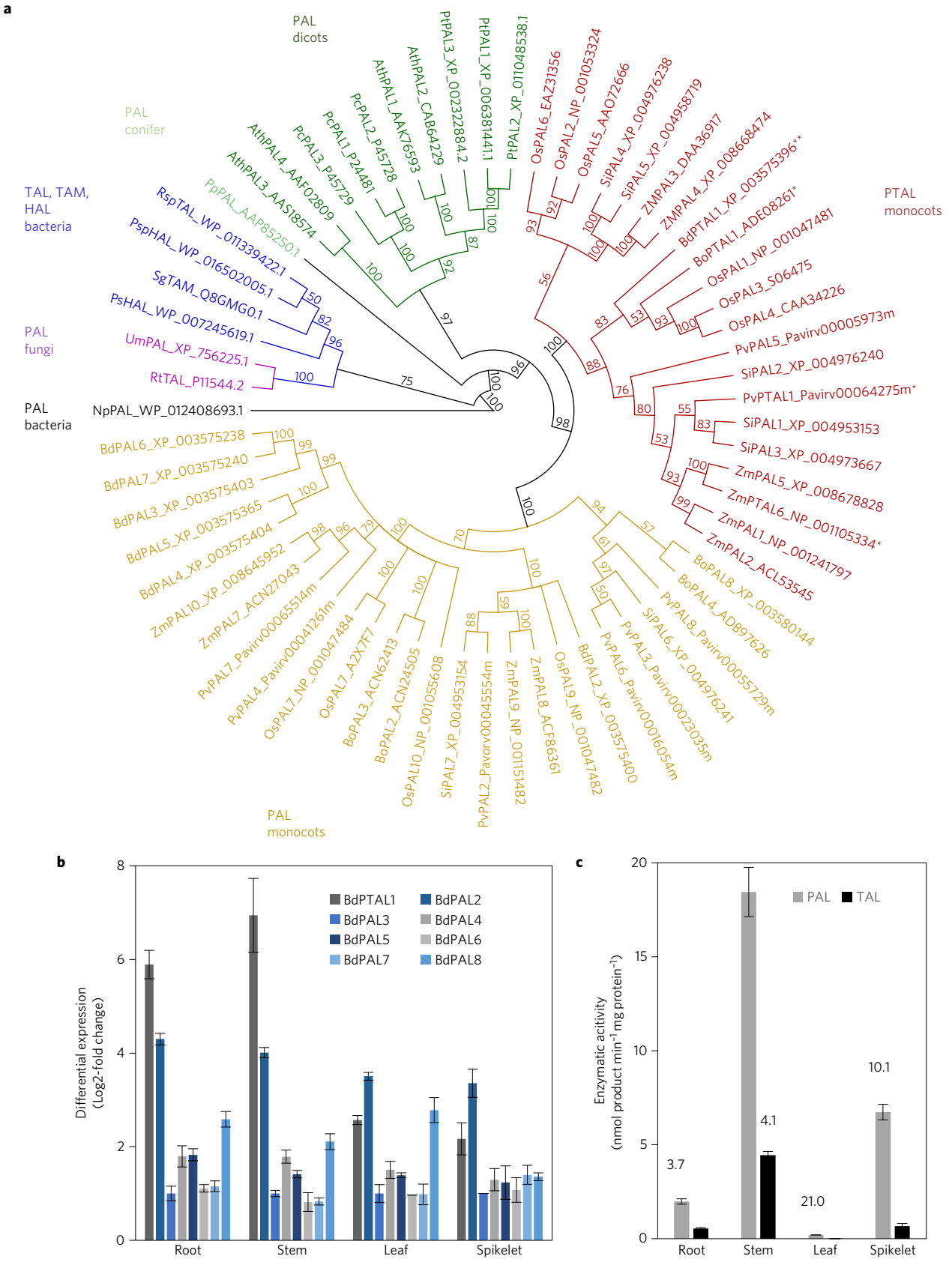

Figure 1 | Phylogeny, gene expression and enzymatic activity of *Brachypodium* BdPALs. a, Phylogenetic tree of PTAL and PAL in plants and fungi, and TAL, tyrosine ammonia-mutase (TAM) and histidine ammonia-lyase (HAL) in bacteria. Protein sequences were obtained from GenBank. *Previously reported PTAL proteins; **PTAL protein characterized in the present study. **b**, Transcript levels of *PALs* in different organs of 30-days-old *Brachypodium* plants as determined by qRT–PCR. **c**, PAL and TAL enzymatic activities determined in the same organ samples as indicated in **b**. Numbers in the top on the bars indicate the average PAL/TAL activity ratio for each organ. Data are mean ± s.e.m., $n > 15$ plants.

Table 1 | Kinetic parameters of recombinant *Brachypodium* PALs and PTAL1 enzymes.

Substrate	K_m (μM)	V_{max} (nkat mg protein^{-1})	K_{cat} (s^{-1})	K_{cat}/K_m (s^{-1} mM^{-1})
L-Phenylalanine				
BdPTAL1*	201.2 ± 85.9	7.1 ± 1.75	0.56	2.8
BdPAL2	31.3 ± 11.8	2.2 ± 0.44	0.18	5.8
BdPAL3	43.9 ± 11.2	4.5 ± 0.68	0.36	8.2
BdPAL4	31.3 ± 15.8	2.0 ± 0.54	0.16	5.1
BdPAL5	26.8 ± 7.5	1.6 ± 0.24	0.13	4.9
BdPAL6	39.8 ± 11.6	4.5 ± 0.76	0.36	9.1
BdPAL7	37.3 ± 6.7	2.6 ± 0.20	0.20	5.4
BdPAL8	61.7 ± 5.1	14.8 ± 0.79	1.20	19.5
L-Tyrosine				
BdPTAL1*	11.9 ± 1.70	0.85 ± 0.05	0.07	5.9
L-DOPA				
BdPTAL1	124.4 ± 20.9	0.63 ± 0.02	0.05	0.4

Enzyme kinetics determined with 500 ng of purified recombinant enzymes incubated with 100 mM Tris-HCl (pH 8.5) and a range of concentrations of L-Phe, L-Tyr or L-DOPA in a total volume of 100 μl. K_m is the Michaelis constant, V_{max} is the maximal rate of the reaction, K_{cat} is the enzyme turnover number and K_{cat}/K_m is the catalytic efficiency. Reactions were carried out at 37 °C for 30 min and terminated by addition of 6 N acetic acid (10 μl).
*PAL and TAL reactions were also carried out with the partially purified BdPTAL1 fractions from *Brachypodium* stem tissues (Fig. 2d) yielding K_m = 266.6 ± 100.1 and V_{max} = 6.7 ± 2.44 for PAL, and K_m = 7.5 ± 2.05 and V_{max} = 1.33 ± 0.37 for TAL reactions with the native enzyme.

BdPTAL1 and all seven *BdPAL* genes are expressed under certain conditions based on transcript data in publicly available gene expression databases (PlaNet http://aranet.mpimp-golm.mpg.de/index.html; Supplementary Fig. 4). However, only *BdPTAL1* and *BdPAL2* showed substantial expression in all tissues examined (Supplementary Fig. 4), and this was further confirmed by quantitative PCR with reverse transcription (qRT–PCR analysis) (Fig. 1b), consistent with previous studies[19]. Transcript levels for *BdPTAL1* (presumed bifunctional) and *BdPAL2* (presumed monofunctional) were higher in lignified tissues (roots and stem) than in less lignified tissues (leaves or spikelet) (Fig. 1b). TAL enzymatic activity was higher in extracts from lignified tissues (roots and stem) than in leaves (Fig. 1c), and the PAL/TAL ratio was higher in mature leaves (21-fold) and spikelets (10-fold) than in lignified tissues such as roots and stems (both by approximately 4-fold) (Fig. 1c), suggesting that TAL could contribute to lignification in vascular tissues.

All eight *Brachypodium* ammonia-lyases were expressed as His-tagged fusion proteins in *Escherichia coli* (Supplementary Fig. 5). All recombinant proteins showed PAL activity, but only BdPTAL1 was a PTAL enzyme with additional TAL activity (Table 1). The Michaelis constant, K_m, value of BdPTAL1 toward L-Phe was 201 μM (the highest value among all BdPALs), whereas the K_m value of BdPTAL1 towards L-Tyr was 17 times lower than that towards L-Phe, indicating a much higher affinity for L-Tyr than for L-Phe. The catalytic efficiency (K_{cat}/K_m) of BdPTAL1 was 2-fold higher towards L-Tyr than towards L-Phe, the former value being similar to that of the monofunctional and highly expressed *BdPAL2* towards L-Phe, and the kinetics of the recombinant BdPTAL1 were similar to those of the purified native enzyme (Table 1). These results indicate that L-Tyr is the preferred substrate of BdPTAL1. This preference was further addressed by assays in the presence of mixed substrates. The TAL activity of BdPTAL1 was high even at low concentrations of L-Tyr (30–50 μM) and with a L-Phe concentration of 250 μM (Supplementary Fig. 6a, left), and was maintained at concentrations of L-Phe approaching 500 μM and constant L-Tyr concentration of 50 μM (Supplementary Fig. 6a, right). Increasing the concentration of L-Tyr in PAL activity assays or L-Phe in TAL activity assays decreased both K_m and the maximal rate of reaction, V_{max} (Supplementary Table 2 and Supplementary Fig. 6b). The observed rates of product formation for BdPTAL1 in the presence of both substrates closely matched those predicted by the single-site model (Supplementary Fig. 6c), which is consistent with a previous study[15] suggesting that PAL and TAL activities share the same active centre. Cinnamic acid inhibited the TAL activity of BdPTAL1, and the PAL activity of both bifunctional and monofunctional PALs (BdPTAL1 and BdPAL2); however, 4CA inhibited both PAL and TAL activities of BdPTAL1 but had no impact on PAL activity of monofunctional BdPALs (Supplementary Fig. 7). Together these results support the contention that grass PTALs are efficient TAL enzymes that will preferentially deaminate L-Tyr *in vivo*. Interestingly, BdPTAL1 also exhibits ammonia-lyase activity (LAL) against the α-amino-acid L-DOPA (3,4-dihydroxyphenylalanine, also known as levodopa), to form caffeic acid. This reaction could theoretically provide for an alternative pathway to the caffeate moiety that would bypass the reactions that take place at the shikimate ester level, and requires use of one less molecule of ATP (Supplementary Fig. 1). However, although the V_{max} values for deamination of L-Tyr and L-DOPA were similar, the kcat/K_m value of the recombinant BdPTAL1 towards L-DOPA was seven times lower than the value for L-Phe and 15 times lower than the value for L-Tyr (Table 1 and Supplementary Fig. 8a). Subcellular fractionation showed that all PAL, TAL and LAL enzymatic activities were mainly detected in the cytosolic fraction, with residual activity in the plastid/microsomal fraction (Supplementary Fig. 8b).

Previous studies have indicated the potential for PAL to exist in heterotetrameric forms[20,21]. The association of BdPTAL1 subunits with other BdPAL subunits would considerably complicate the assessment of the function of TAL. The subunit composition of BdPTAL1 protein(s) was therefore determined. The recombinant BdPTAL1 subunit migrated on SDS–polyacrylamide gel electrophoresis (SDS–PAGE) gel with an apparent molecular mass of 77 kDa (Fig. 2a, left and Supplementary Fig. 5). Using gel filtration chromatography on Toyopearl HW-55S resin, the molecular mass of native *Brachypodium* stem PTAL1 was estimated to be about 290 kDa (Fig. 2a, right), indicating that native BdPTAL1 exists as a tetramer. To determine if native *Brachypodium* stem PTAL1 is a homo- or heterotetramer, we subjected crude enzyme extracts from stems to sequential purification by ammonium sulfate fractionation, gel filtration and anion exchange chromatography (Fig. 2b–d; Supplementary Table 3). Monofunctional PAL activity was observed in the 0–40% ammonium sulfate fractions whereas later fractions (40–80%) showed both PAL and TAL activities (Fig. 2b), indicating the coexistence of monofunctional PALs and bifunctional PTAL in *Brachypodium*, with lower solubility of the former. The 30–40%, 40–50% and 50–60% ammonium sulfate fractions were loaded on the gel filtration column (Fig. 2c) and the fraction with highest TAL activity (peak 6 from the 50–60% fraction) was subsequently loaded on a MonoQ HR 5/5 anion exchange column (Fig. 2d). PTAL activity was eluted between

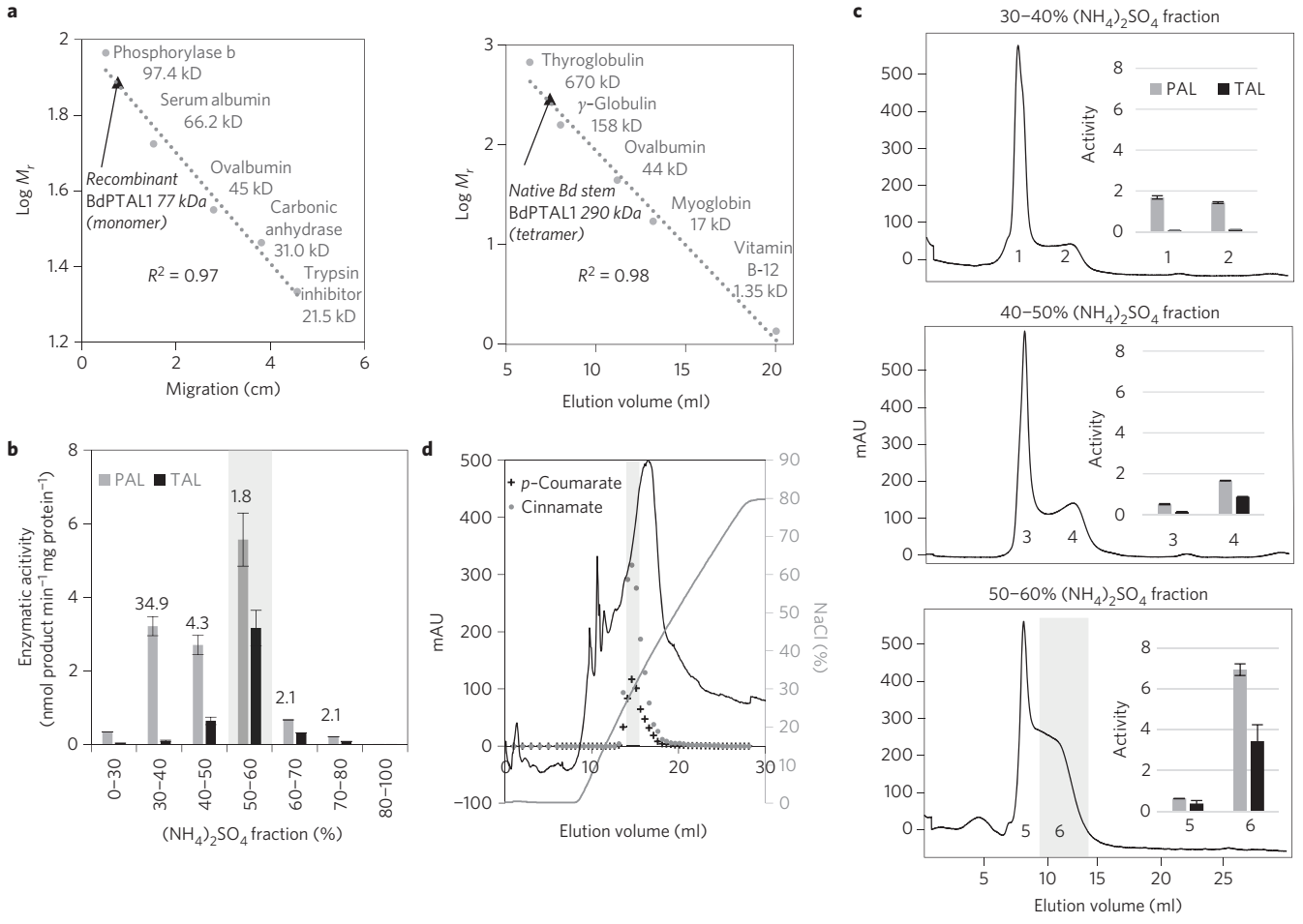

Figure 2 | Purification of the native PTAL enzyme from *Brachypodium* stem tissue. a, Subunit molecular mass of recombinant BdPTAL1 determined by 10% SDS–PAGE (left) and molecular mass of native BdPTAL1 from stem extracts determined by gel filtration chromatography on Toyopearl HW-55S (right). **b**, PAL and TAL enzymatic activities in different ammonium sulfate fractions prepared from a crude stem protein extract. Numbers represent the PAL/TAL ratios. **c**, Enzymatic activities and fast protein liquid chromatography (FPLC) profile obtained from the different ammonium sulfate fractions (30–40%, 40–50% and 50–60%) purified by gel filtration (Toyopearl HW-55S). Peaks observed in the FPLC profile were combined and PAL and TAL activities determined in fractions from 1 to 6. **d**, Enzymatic activities and FPLC profile obtained from the 50–60% ammonium sulfate fraction purified using a MonoQ HR5/5 column. The fraction #6 with higher TAL activity obtained from **c** was loaded in the ion exchange column for further purification and subjected to protein identification with ESI–MS/MS. Fractions collected for determination of the protein subunit composition are indicated as grey shaded areas (see also Supplementary Table 3). Data presented in bar charts are mean ± s.e.m., $n = 3$.

30% and 35% NaCl and the overall PAL/TAL ratio in the purified fractions (grey shaded area in Fig. 2d) was 2.9 ± 0.5, compared with 3.9 ± 0.1 for recombinant BdPTAL1 (Supplementary Table 4), indicating that expression of recombinant enzyme *in vitro* had a negative impact on the relative TAL activity. The purified *Brachypodium* stem PTAL protein was subjected to SDS–PAGE followed by protein sequencing, in parallel with recombinant BdPTAL1 as control. The 20 peptides found matched the sequence of BdPTAL1, covered about 35% of the sequence and were all found in the recombinant purified BdPTAL1 with none being BdPAL-specific (Supplementary Table 4), indicating that BdPTAL1 forms homotetramers *in vivo*.

Previous literature[13,15] supports the participation of PTAL in phenylpropanoid biosynthesis. To further investigate PTAL function, we performed isotopic tracing of phenylpropanoid biosynthesis using $^{13}C_9$ labelled precursors (Fig. 3), and also generated *BdPTAL1* RNA interference (RNAi) lines of *Brachypodium distachyon* to study the impact of disruption of *PTAL* expression on cell wall lignification (Fig. 4). We first grew *Brachypodium* plants on media containing either $^{13}C_9$-labelled L-Phe or L-Tyr, harvested them at 10 and 30 days after germination and analysed their lignin compositions by thioacidolysis gas chromatography mass spectrometry (GC–MS). Fifteen-day-old *Arabidopsis* plants were used for comparison. The extent of labelling of the L-Phe and L-Tyr pools was similar (around 35%) and not affected by the co-application of 4CA or cinnamic acid (Supplementary Fig. 9a, left). Following mass spectrometry, unlabelled thioacidolysis products of H, G and S monolignols were detected at m/z 239, 269 and 299, respectively, and labelled units were identified at increased molecular mass of [M+7] = 246, 276 and 306, respectively, as would be predicted from incorporation of nine labelled carbons followed by loss of two carbons during mass spectrometry fragmentation (Supplementary Fig. 10). Only the plants fed with labelled precursors exhibited M+7 monolignol-derived fragmentation products and, consistent with their degree of lignification and the method of label application, label incorporation into monolignol units was better in roots than in stems (Fig. 3a). Incorporation of label was similar in 10-day-old plantlets and 30-day-old plants (Fig. 3a). L-Phe was preferentially incorporated into the H-units of lignin in root tissues at both developmental stages, whereas L-Tyr was somewhat better incorporated into the S-units. As expected, based on the lack of TAL activity, 15-day-old *Arabidopsis* roots incorporated only

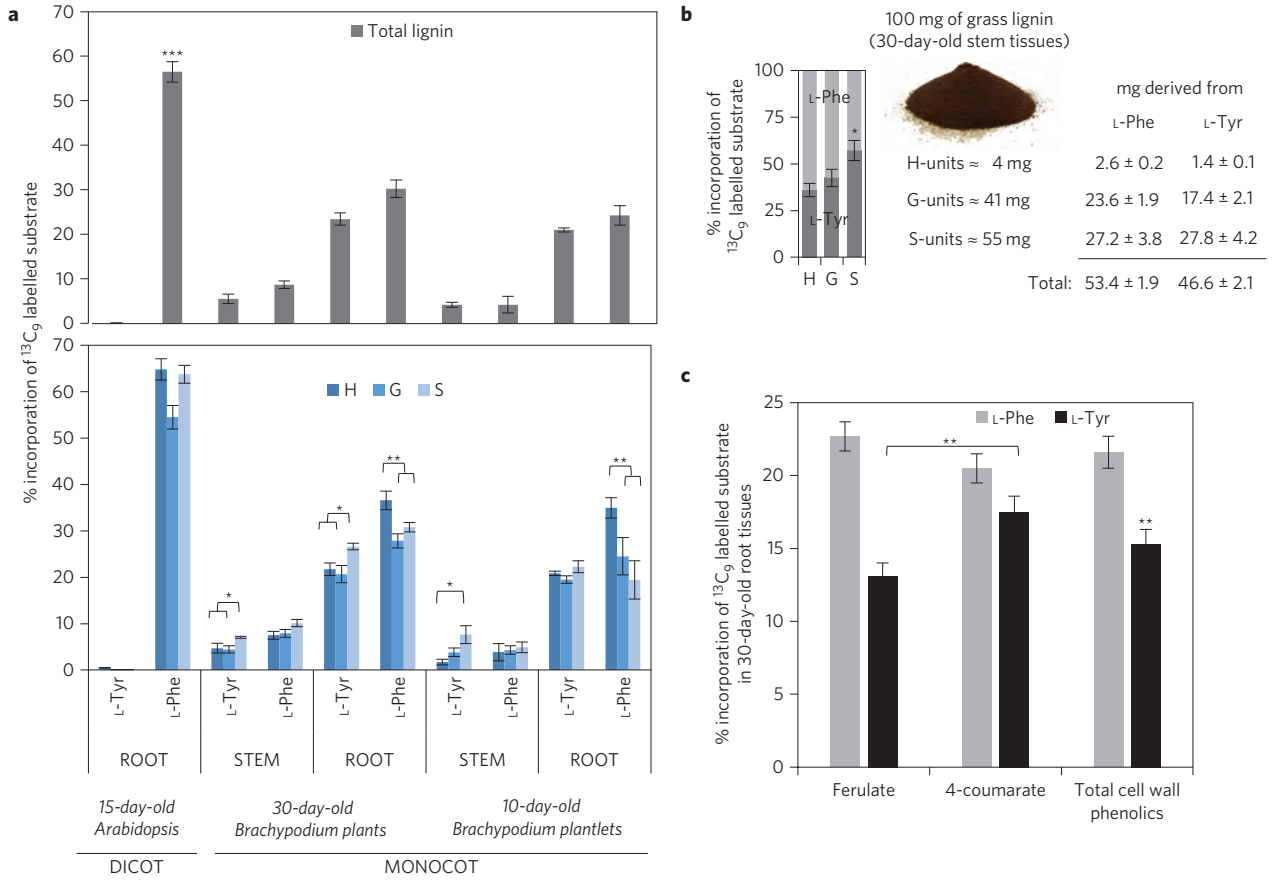

Figure 3 | Labelling of *Brachypodium* seedlings with $^{13}C_9$-L-Phe and $^{13}C_9$-L-Tyr. a, Percentage of ^{13}C label incorporated into lignin in root and stem tissues of *Brachypodium* and *Arabidopsis* plants grown on media containing either $^{13}C_9$-labelled L-Phe or L-Tyr for 10, 15 or 30 days as indicated. In the lower panel, the percentage values refer to the labelled percentage of the individual lignin monomers. **b**, Estimation of lignin composition derived from L-Phe and L-Tyr based on the above labelling experiments for *Brachypodium* stem tissues grown on media containing labelled substrates for 30 days. **c**, Percentage incorporation of labelled precursors into cell wall-esterified phenolic acids released from lignin and hemicellulose with 1M NaOH in root tissues of *Brachypodium* plants fed with labelled L-Phe or L-Tyr for 30 days. The asterisks indicate significant differences at the $*p < 0.05$ and $**p < 0.01$ levels; unpaired two-sided *t*-test. Data are represented as mean ± s.e.m., $n > 20$ plants.

L-Phe into lignin (Fig. 3a, lower panel). Considering the above labelling experiments for *Brachypodium* stems grown on media containing labelled substrates for 30 days, and the proportional abundance of each lignin monomer determined in wild-type plants (see Fig. 4b, right), we estimate that 100 mg of lignin from *B. distachyon* stem tissues contain on average 4 mg of H-units (3 mg synthesized from L-Phe and 1 mg from L-Tyr), 41 mg of G-units (24 mg derived from L-Phe and 17 mg from L-Tyr) and 55 mg of S-units (27 mg derived from L-Phe and 28 mg from L-Tyr) (Fig. 3b). It should be noted that these values are based on thioacidolysis yields, which reflect the proportion of lignin units that are joined by the majority β-*O*-4 linkages. Thus, whereas dicot plants synthesize all their lignin monomers from L-Phe, the TAL activity of PTAL can provide nearly half of the lignin monomers observed in grasses, with a slight preference for S-monolignol biosynthesis.

Unlike dicots, grasses contain significant amounts of esterified 4CA and ferulate in their cell walls[22,23]. $^{13}C_9$-label was also detected in these molecules, with significantly better incorporation of L-Tyr into 4CA than into ferulate (Fig. 3c). Isotope dilution/inhibitor assays were performed to further examine the pathways of monolignol biosynthesis in *Brachypodium* (Supplementary Fig. 9). Addition of cinnamic acid in the medium at 100 μM completely blocked incorporation of label from L-Phe into lignin, but only partially inhibited incorporation of L-Tyr (Supplementary Fig. 9b), consistent with both or either enzyme inhibition and/or isotope dilution of the cinnamic acid pool, since PAL and TAL activities of mono- and bifunctional BdP(T)ALs are equally inhibited by cinnamic acid (Supplementary Fig. 5c). However, 4CA (500 μM) only significantly inhibited incorporation of label from L-Tyr; this compound inhibits both PAL and TAL activities of BdPTAL1 but does not inhibit BdPALs (Supplementary Fig. 5c). Importantly, this observation indicates that unlabelled 4CA does not dilute the pool of labelled 4CA derived from L-Phe, whereas it may dilute the pool derived from L-Tyr. Growth of plants in the presence of cinnamic acid (to reduce flux from L-Phe) resulted in increased lignin S/G ratios, whereas plants grown in the presence of 4CA (to reduce flux from L-Tyr) resulted in reduced levels of S-units in lignin (Supplementary Fig. 9c), as well as favouring the incorporation of L-Phe into wall-bound ferulate and reducing the incorporation of L-Tyr into wall-bound 4CA (Supplementary Fig. 9d). Taken together, these experiments provide support for distinct metabolic pools (of 4CA and possibly other upstream metabolites) associated with the PAL and TAL pathways.

To provide genetic evidence to confirm the conclusions of the above labelling studies, *BdPTAL1* expression was downregulated using an RNAi strategy with the silencing RNA under the control of the ZmUbi1 promoter that is expressed in most tissue types during most stages of grass development[24]. *BdPTAL1i* plants showed a wild-type visual phenotype without developmental abnormalities (Fig. 4a), although plants in which both BdPTAL1

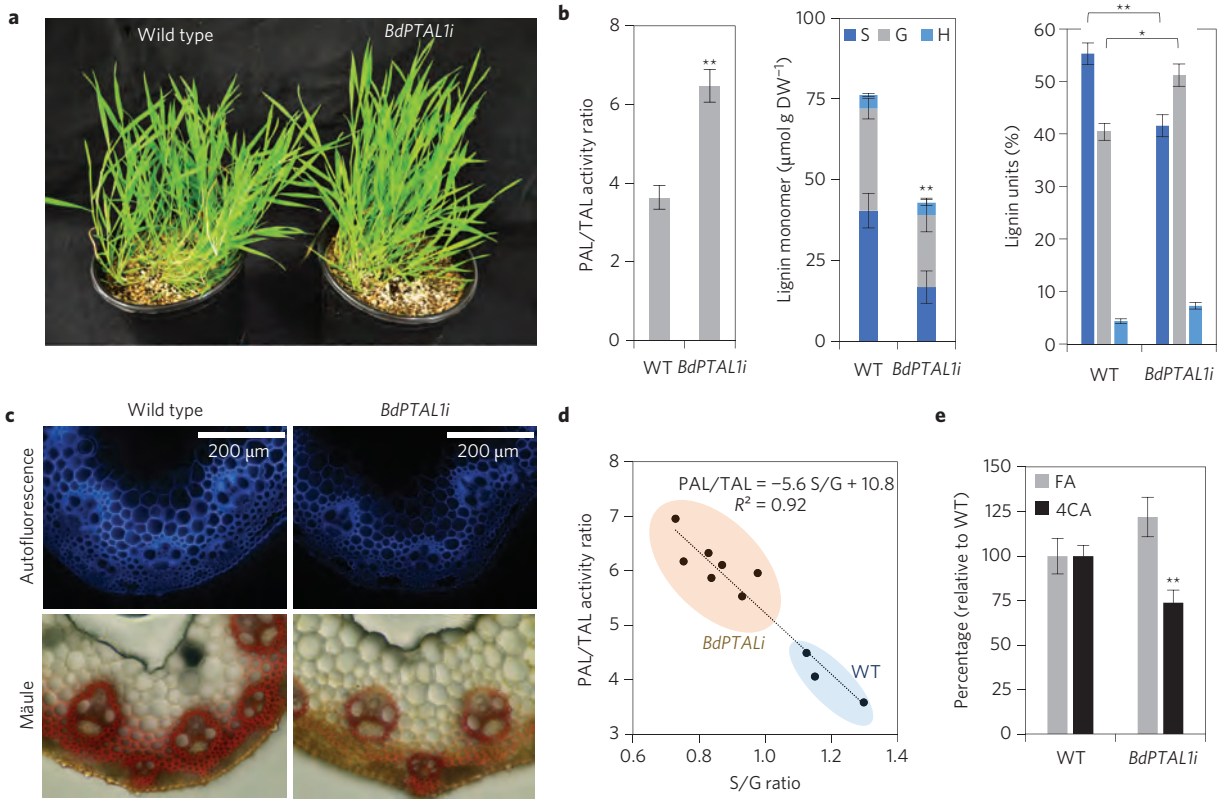

Figure 4 | Phenotype and lignin characteristics of *Brachypodium PTAL1* RNAi lines. a, Fully grown wild-type and *BdPTAL1i* (line #25) *Brachypodium* plants. **b**, PAL/TAL activity ratio and lignin levels and composition determined by thioacidolysis for three controls and seven independent lines: BdPTAL1i-3, 9, 12, 22, 25, 26 and 27 (see Supplementary Fig. 11 for more details). **c**, Transverse stem sections of *Brachypodium BdPTAL1*i (line #25) and corresponding wild-type plant. Mäule staining (lower panels) and lignin ultraviolet autofluorescence (upper panels). Scale bar, 200 μm. **d**, Simple linear correlation and adjusted equation between extractable PAL/TAL activity ratios and lignin S/G ratio for the same plants as indicated in **b**. **e**, Levels of cell wall-bound phenolics (FA, ferulate and 4CA, 4-coumarate) for the same plants as indicated in **b**. $^{**}p < 0.01$; $^{*}p < 0.05$; unpaired two-sided *t*-test. Error bars represent s.e.m., $n = 7$ plants.

and BdPAL2 were downregulated have been reported to exhibit altered flowering time and root growth[19]. *BdPTAL1* transcript levels analysed by qRT–PCR were on average reduced to 30% of wild type, with the reduction in some lines being as much as to 6% of wild type; however, many transgenic lines also showed some downregulation of monofunctional *BdPAL* transcript levels (Supplementary Fig. 11a). We selected seven *BdPTAL1* downregulated lines with the lowest levels of *PAL* gene downregulation (Supplementary Fig. 11a), and confirmed the biochemical phenotypes by measurement of overall PAL and TAL activities in crude protein extracts, lignin monomer composition, and levels of wall-bound coumaric and ferulic acids (Supplementary Fig. 11b). Increased PAL/TAL ratio of the *BdPTALi* lines led to a 43% reduction in thioacidolysis-quantified lignin monomer units due to a predominant reduction in S-unit deposition (Fig. 4b). Analysis of transverse sections of *BdPTAL1i* stems revealed reduced autofluorescence and less intense and altered Mäule staining in vessels and fibres, indicative of reduced lignin content and fewer S-units (Fig. 4c). The S/G ratio was strongly correlated with the PAL/TAL ratio ($R^2 = 0.92$) in the seven *BdPTALi* lines analysed (Fig. 4d), and the fraction of cell wall bound 4CA released by alkaline hydrolysis was reduced by 26% in the *BdPTAL1i* plants compared with wild-type controls (Fig. 4e). Four independent lines with the PAL expression levels upregulated or unchanged (lines #9, 22, 25 and 27, Supplementary Fig. 11a) were selected for subsequent metabolic profiling using liquid chromatography mass spectrometry. Principal component analysis revealed a clear differentiation of *BdPTAL1i* lines from wild-type controls (Supplementary Fig. 12a). Levels of soluble 4CA and some flavonoids were reduced in *BdPTAL1i* lines, whereas ferulate, chlorogenic acid (CGA) and quinic acid levels were increased by ≥1.5-, 2- and 4-fold, respectively (Supplementary Fig. 12b). We believe that the above effects on S/G ratio and metabolite levels are due to the change in PAL/TAL ratio as a result of reduction in TAL activity, rather than reduction of the associated PAL activity of bi-functional PTAL, because the kinetic properties of the enzyme suggest that it is unlikely to function as a PAL *in vivo*. We therefore conclude that BdPTAL1 is preferentially involved in the biosynthesis of S-units and wall bound 4CA in planta, but is not preferentially involved in the biosynthesis of chlorogenic acid.

Discussion

The reason why grasses have retained the capacity for tyrosine deamination through their possession of TALs is an unresolved question in plant biochemistry. We have now addressed the role of bifunctional ammonia-lyase in phenylpropanoid biosynthesis in the model grass *Brachypodium distachyon*. Although only one of the eight genes annotated as a *BdPAL* in *B. distachyon* encodes a bifunctional PAL/TAL, and PAL activity is significantly higher than TAL activity in both crude extracts and as computed from kinetic values for the eight recombinant enzymes, L-Tyr is nearly as efficiently incorporated into lignin as is L-Phe. Compared to L-Phe, L-Tyr is preferentially incorporated into the S-units of lignin, as well as into cell wall bound 4CA. These findings indicate that grass PTALs contribute significantly to the special characteristics of grass cell walls (Fig. 5), but do not yet explain exactly how this occurs. Several mechanisms are possible. For example, our labelling

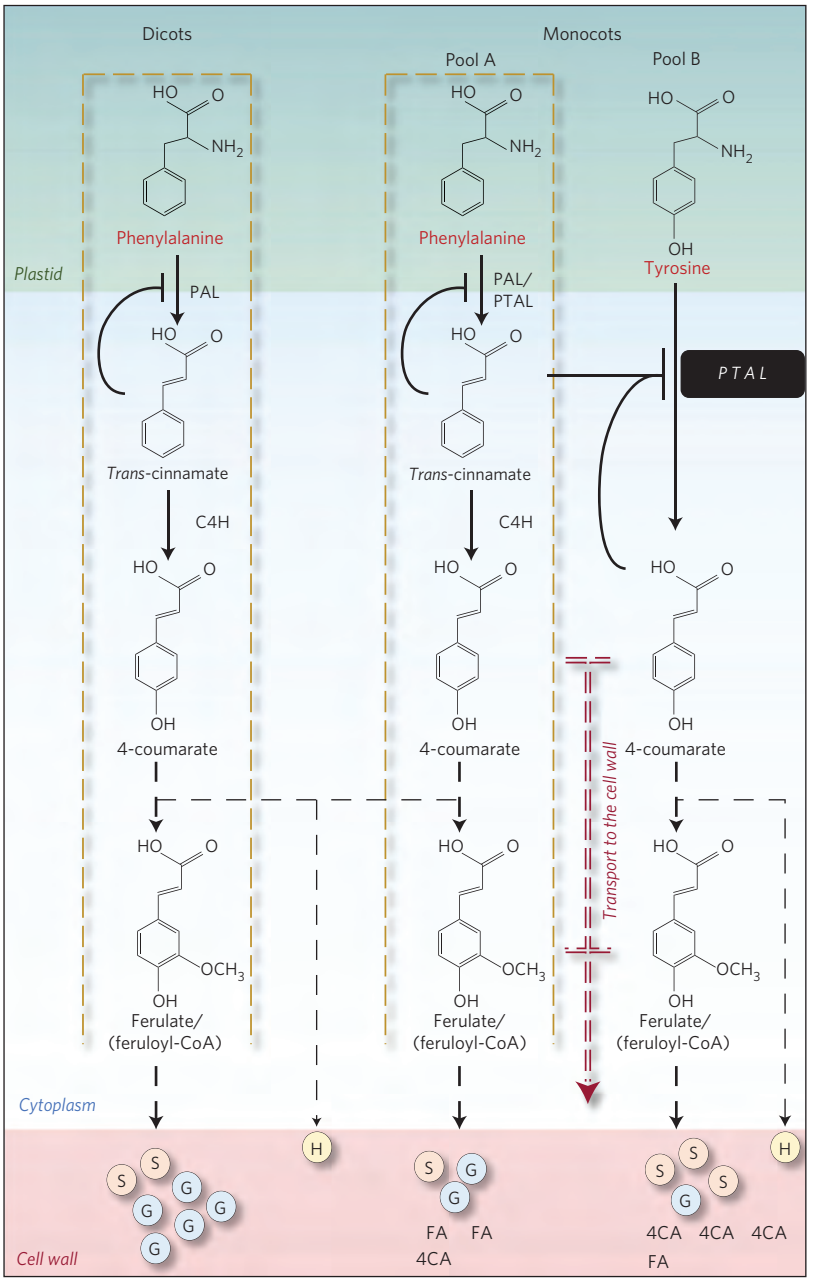

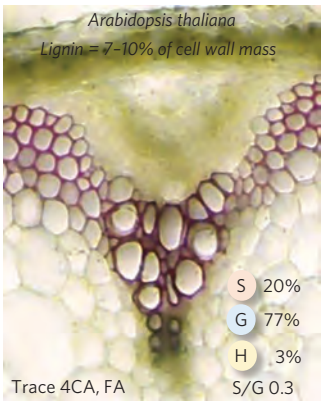

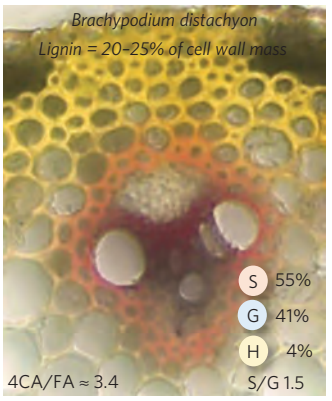

Figure 5 | Model for the early steps of lignin synthesis including both PAL and TAL pathways in monocot plants. Inhibition is indicated by lines with bars. Dashed arrows represent abbreviated biosynthetic steps. The brown dashed boxes represent putative metabolic channels. Note that it is not clear at what point the fluxes from L-Tyr and L-Phe meet. FA, ferulate; 4CA, 4-coumarate; C4H, cinnamate 4-hydroxylase; S, G and H: syringyl, guaiacyl and *p*-hydroxyphenyl units of lignin.

studies suggest that the pathway to lignin and wall bound 4CA from L-Tyr is distinct from the formation of these compounds via L-Phe, raising the question of whether the parallel pathways feature distinct enzymatic activities or common enzymes in different metabolic channels. The major cell biological distinction between the formation of 4CA from L-Phe or L-Tyr is the fact that the 4CA formed via L-Phe is generated by C4H, a cytochrome P450 enzyme that is bound to the outer face of the endoplasmic reticulum where it has been proposed to function in the assembly of a metabolic channel for monolignol synthesis[25–27], and possibly additional channels leading to the formation of other classes of phenylpropanoid-derived compounds such as flavonoids[28]. The presence of such channels in *Brachypodium* is suggested by the inability of exogenously supplied 4CA to dilute incorporation of label from L-Phe, but not from L-Tyr, into lignin. 4CA formed directly from L-Tyr by the activity of TAL may avoid entry into such channels. The question then arises as to whether the subsequent reactions in the lignin pathway from 4CA derived from L-Tyr are identical to those involved in the conversion of 4CA derived from L-Phe. It seems unlikely that these reactions would be divergent beyond the formation of coniferaldehyde. However, the effects of PAL/TAL ratio on lignin S/G ratio could theoretically reflect kinetic effects at the branch point between G and S lignin synthesis. The potential for parallel pathways is currently being addressed by genetic loss of function experiments. The distinctive role of PTAL might also be associated with differential cell type-specific expression and/or differential availabilities of L-Phe and L-Tyr.

According to the currently favoured pathway to monolignols[29], the formation of caffeic acid from L-Phe involves six enzymatic steps, catalysed by PAL, C4H, 4-coumarate:CoA ligase (4CL), hydroxycinnamoyl CoA:shikimate hydroxycinnamoyl transferase (HCT), coumaroyl shikimate 3′-hydroxylase (C3′H) and caffeoyl shikimate esterase (CSE). Theoretically, this pathway could be simplified to a two-step pathway from L-Tyr through the action of a tyrosine hydroxylase to generate DOPA, and, as demonstrated in the present work, LAL to convert DOPA to caffeic acid, with the LAL activity being a property of PTAL1. Direct evidence for such a pathway is currently lacking, because tyrosine hydroxylase activity is found in plants of the order Caryophyllales, where it is involved in the synthesis of betalain pigments[30], but has yet to be reported from grasses, and labelling studies with L-DOPA are problematic because of the toxicity and ready oxidation of the compound. Genetics-based investigations into the possible operation of this alternative pathway in *Brachypodium* are ongoing.

Metabolic profiling of *BdPTAL1* downregulated plants also revealed reductions in the pools of several flavone and flavonol derivatives, indicating that the TAL pathway also provides substrates for flavonoid biosynthesis. This pathway diverges from monolignol synthesis at the level of coumaroyl CoA. Further labelling studies will be necessary to determine whether there are differential roles for PAL and PTAL in flavonoid biosynthesis. The position of PTAL at the interface of primary and secondary metabolism suggests that manipulation of PTAL in grasses might also impact primary metabolism, as observed here by the increased levels of quinic acid (and its ester chlorogenic acid) in BdPTAL1 downregulated plants.

Methods

Phylogenetic analysis. Amino acid multiple sequence alignments were created using Geneious 8.0.4 software (Biomatters Ltd) with default settings and are presented in Supplementary Fig. 2. The phylogenetic tree was built by Geneious Pro 5.5.6 with PHYML plugin[31,32], that uses a maximum likelihood algorithm, as described in Supplementary Methods.

Plant material and growth conditions. *B. distachyon* community standard inbred line Bd21-3 was grown under a 16-h light/8-h dark photoperiod at 100 μE m^{-2} s^{-1} at 22 °C and harvested at 30 d after germination to prepare protein crude extracts from the different plant organs.

RNA isolation and qRT–PCR. RNA isolation and determination of transcript levels by qRT–PCR are described in Supplementary Materials.

Expression and purification of recombinant BdPALs. Full length complementary DNA sequences found in the NCBI public database were used for primer design to clone target genes. cDNA synthesis is described in Supplementary Materials. Open reading frames were amplified by PCR using Phusion High-Fidelity DNA polymerase (New England Biolabs), and cloned into the expression vector pDEST17 using the Gateway technology (Invitrogen). The primers used for cloning are listed in Supplementary Table 6. Plasmids were isolated using the QIAprep DNA Purification Kit (Qiagen), and their insert cDNAs were sequenced in both directions for verification. LR reactions were performed using *BdPALs* cloned into the pENTR/D-TOPO vector with pDEST17 (Invitrogen), which provides a 6× Histidine tag at the N terminus of the expressed target gene to facilitate protein purification, as described in Supplementary Methods.

Enzyme assays. PAL and TAL activities were assayed by measuring *trans*-cinnamic acid and *p*-coumaric acid formation by HPLC as previously reported[33] with some modifications, as described in Supplementary Methods.

Electrophoresis. The molecular mass of the single BdPTAL1 monomer subunit was determined by sodium dodecyl sulfate polyacrylamide gel electrophoresis as described in Supplementary Methods. After purification of native *Brachypodium* PTAL1 protein from plant stems (see below), the molecular mass of the multimer was estimated by gel filtration chromatography, as described in Supplementary Methods.

Purification of native BdPTAL1 protein. BdPTAL1 was purified from mature stem tissues by a combination of ammonium sulfate precipitation, gel filtration and ion exchange chromatography as described in Supplementary Methods.

Protein identification with electrospray ionization tandem mass spectrometry (ESI–MS)/MS. The pure BdPTAL1 enzyme preparation from stems was subjected to electrophoresis and the gel stained with Coomassie Brilliant Blue R-250. The main protein band was excised for in-gel digestion[34] and peptide mass mapping as described in Supplementary Methods.

Plant transformation. Generation of a BdPTAL1 RNAi construct targeting the *Brachypodium* Bd3g49250.2 gene transcript and transformation with this construct are described in Supplementary Methods.

Measurement of lignin content and composition. Cell wall residues were prepared by sequentially extracting *Brachypodium* stems with chloroform/methanol (1:1), 100% methanol, 50% methanol and water for three times each at room temperature. Fifteen milligrammes of lyophilized samples were used for lignin analysis. Total lignin content and monomer composition were determined by thioacidolysis followed by GC–MS as previously described[35].

Determination of incorporation of ^{13}C into amino acids, lignin and hydroxycinnamates. For the labelling experiments, *Brachypodium* and *Arabidopsis* plants were grown in culture tubes containing 1× Murashige and Skoog salt mixture, 3% sucrose (pH 5.8) in 0.5% Phytagel fed with 0.1 mM $^{13}C_9$-L-Tyr and $^{13}C_9$-L-Phe (Cambridge Isotope Laboratories) under continuous light conditions and harvested at 10, 15 and 30 days after germination as indicated in the figures. Experiments using unlabelled lignin precursors were conducted in parallel. The plants were separated into root, stem and leaf fractions which were stored at −80 °C until use. The percentage of label incorporated into each compound was calculated as:

$$\%^{13}\text{C incorporated} = \text{peak area labelled}/(\text{peak area labelled} + \text{peak area unlabelled}) \times 100.$$

To determine how much of the total pool size of precursors was labelled (Supplementary Fig. 7a), the amino acids L-Phe and L-Tyr in the polar extracts were measured by GC–MS as previously described[36]. Peak areas of the thioacidolysis products of lignin (H-, G- and S-units) were identified as indicated above, and the incorporation into total lignin was estimated using the sum of the three individual peak areas. The methods used for identification of the cell wall-bound hydroxycinnamates ferulate and 4-coumarate are described below.

Microscopy. Stems from fully grown but still green plants (*Brachypodium*: 16-h light/8-h dark photoperiod at 22 °C harvested at 35 days after germination; *Arabidopsis*: 9-h light/15-h dark at 22 °C for eight weeks, followed by 16-h light/8-h dark, 22 °C for four weeks) were cut and the bottom 2 cm was embedded in 7% agarose. Slices (100 μm thick) were cut with a Vibratome (Campden Instruments, UK) and Mäule stained as previously reported[37] with slight modifications as described in Supplementary Methods.

Quantification of cell wall bound and soluble phenolics. Wild-type and *BdPTAL1*-RNAi plants ($n = 4$) were grown and stems harvested as described above. Twenty milligrammes of extractive-free cell wall residues were used for analysis of esterified

cell wall-bound phenolics using low-temperature alkaline hydrolysis (2 M NaOH, 37 °C, 5 h)[38], as described in Supplementary Methods. For determination of soluble phenolics, 10 mg of powdered plant material was homogenized and extracted in 1 ml of 80% methanol containing 0.018 mg ml^{-1} umbelliferone (internal standard) at room temperature for 2 h on an orbital shaker. After centrifugation, 5 µl of supernatant was analysed by ultra performance liquid chromatography coupled to both photodiode array and mass spectrometry detection. Mass spectra were acquired in the negative electrospray ionization mode on a hybrid quadrupole time-of-flight mass spectrometer as previously described[39]. Principal component analysis was performed in XLSTAT (Addinsoft).

Statistical analyses. Asterisks on tables and tops of bars indicate values that were determined by Student's *t*-test (Microsoft Office Excel 2007) to be significantly different from the equivalent controls (*, **, ***, indicate $p < 0.05$, 0.01 and 0.001, respectively).

Accession codes. Genbank. The accession numbers for the *Brachypodium PTAL* and *PAL* sequences mentioned in this article are as follows: *BdPTAL1*, XM_003575348.1, Bradi3g49250.2; *BdPAL2*, XM_003575352.1, Bradi3g49260; *BdPAL3*, XM_003575355.1, Bradi3g49270.1; *BdPAL4*, XM_003575356.1, Bradi3g49280.1; *BdPAL5*, XM_003575317.1, Bradi3g48840.1; *BdPAL6*, XM_003575190.1, Bradi3g47110.1; *BdPAL7*, XM_003575192.1, Bradi3g47120.1; *BdPAL8*, XM_003580096.1, Bradi5g15830.1.

Received 29 November 2015; accepted 10 March 2016; published 9 May 2016

References

1. Kenrick, P. & Crane, P. R. The origin and early evolution of plants on land. *Nature* **389,** 33–39 (1997).
2. Bateman, R. M. *et al.* Early evolution of land plants: phylogeny, physiology, and ecology of the primary terrestrial radiation. *Annu. Rev. Ecol. Syst.* **29,** 263–292 (1998).
3. Dixon, R. A. *et al.* The phenylpropanoid pathway and plant defence –a genomics perspective. *Mol. Plant Pathol.* **3,** 371–390 (2002).
4. Maeda, H. & Dudareva, N. The shikimate pathway and aromatic amino acid biosynthesis in plants. *Annu. Rev. Plant Biol.* **63,** 73–105 (2012).
5. Vanholme, R. *et al.* Caffeoyl shikimate esterase (CSE) is an enzyme in the lignin biosynthetic pathway in *Arabidopsis*. *Science* **341,** 1103–1106 (2013).
6. Appert, C., Logemann, E., Hahlbrock, K., Schmid, J. & Amrhein, N. Structural and catalytic properties of the four phenylalanine ammonia-lyase isoenzymes from parsley (*Petroselinum crispum* Nym.). *Eur. J. Biochem.* **225,** 491–499 (1994).
7. Kyndt, J. A., Meyer, T. E., Cusanovich, M. A. & Van Beeumen, J. J. Characterization of a bacterial tyrosine ammonia-lyase, a biosynthetic enzyme for the photoactive yellow protein. *FEBS Lett.* **512,** 240–244 (2002).
8. Cochrane, F. C., Davin, L. B. & Lewis, N. G. The *Arabidopsis* phenylalanine ammonia-lyase gene family: kinetic characterization of the four PAL isoforms. *Phytochemistry* **65,** 1557–1564 (2004).
9. Havir, E. A., Reid, P. D. & Marsh, H. V. L-phenylalanine ammonia-lyase (maize) evidence for a common catalytic site for L-phenylalanine and L-tyrosine. *Plant Physiol.* **48,** 130–136 (1971).
10. Rosler, J., Krekel, F., Amrhein, N. & Schmid, J. Maize phenylalanine ammonia-lyase has tyrosine ammonia-lyase activity. *Plant Physiol.* **113,** 175–179 (1997).
11. Jangaard, N. O. The characterization of phenylalanine ammonia-lyase from several plant species. *Phytochemistry* **13,** 1765–1768 (1974).
12. Hsieh, L., Ma, G., Yang, C. & Lee, P. Cloning, expression, site-directed mutagenesis and immunolocalization of phenylalanine ammonia-lyase in *Bambusa oldhamii*. *Phytochemistry* **71,** 1999–2009 (2010).
13. Brown, S. A., Wright, D. & Neish, A. C. Studies of lignin biosynthesis using isotopic carbon: VII.: The role of *p*-hydroxyphenylpyruvic acid. *Can. J. Biochem. Physiol.* **37,** 25–34 (1959).
14. Higuchi, T., Ito, Y. & Kawamura, I. *p*-Hydroxyphenylpropane component of grass lignin and role of tyrosine-ammonia lyase in its formation. *Phytochemistry* **6,** 875–881 (1967).
15. Louie, G. V. *et al.* Structural determinants and modulation of substrate specificity in phenylalanine-tyrosine ammonia-lyases. *Chem. Biol.* **13,** 1327–1338 (2006).
16. Watts, K. T., Mijts, B. N., Lee, P. C., Manning, A. J. & Schmidt-Dannert, C. Discovery of a substrate selectivity switch in tyrosine ammonia-lyase, a member of the aromatic amino acid lyase family. *Chem. Biol.* **13,** 1317–1326 (2006).
17. Rétey, J. Discovery and role of methylidene imidazolone, a highly electrophilic prosthetic group. *Biochim. Biophys. Acta* **1647,** 179–184 (2003).
18. MacDonald, M. J. & D'Cunha, G. B. A modern view of phenylalanine ammonia-lyase. *Biochem. Cell Biol.* **85,** 273–282 (2007).
19. Cass, C. *et al.* Effects of phenylalanine ammonia lyase (PAL) knockdown on cell wall composition, biomass digestibility, and biotic and abiotic stress responses in *Brachypodium*. *J. Exp. Bot.* **66,** 4317–4335 (2015).
20. Reichert, A., He, X. & Dixon, R. A. Phenylalanine ammonia-lyase (PAL) from tobacco (*Nicotiana tabacum*): characterization of the four tobacco PAL genes and active heterotetrameric enzymes. *Biochem. J.* **424,** 233–242 (2009).
21. Hyun, M. W., Yun, Y. H., Kim, J. Y. & Kim, S. H. Fungal and plant phenylalanine ammonia-lyase. *Mycobiology* **39,** 257–265 (2011).
22. Vogel, J. Unique aspects of the grass cell wall. *Curr. Opin. Plant Biol.* **11,** 301–307 (2008).
23. Harris, P. J. & Hartley, R. D. Detection of bound ferulic acid in cell walls of the Gramineae by ultraviolet fluorescence microscopy. *Nature* **259,** 508–510 (1976).
24. Mann, D. G. J. *et al.* Gateway-compatible vectors for high-throughput gene functional analysis in switchgrass (*Panicum virgatum* L.) and other monocot species. *Plant Biotechnol. J.* **10,** 226–236 (2012).
25. Rasmussen, S. & Dixon, R. A. Transgene-mediated and elicitor-induced perturbation of metabolic channeling at the entry point into the phenylpropanoid pathway. *Plant Cell* **11,** 1537–1551 (1999).
26. Achnine, L., Blancaflor, E. B., Rasmussen, S. & Dixon, R. A. Colocalization of L-phenylalanine ammonia-lyase and cinnamate 4-hydroxylase for metabolic channeling in phenylpropanoid biosynthesis. *Plant Cell* **16,** 3098–3109 (2004).
27. Bassard, J.-E. *et al.* Protein–protein and protein–membrane associations in the lignin pathway. *Plant Cell* **24,** 4465–4482 (2012).
28. Winkel, B. S. J. Metabolic channeling in plants. *Annu. Rev. Plant Biol.* **55,** 85–107 (2004).
29. Zhao, Q., & Dixon, R. A. Altering the cell wall and its impact on plant disease: from forage to bioenergy. *Annu. Rev. Phytopathol.* **52,** 62–91 (2014).
30. Yamamoto, K., Nobayashi, N., Yoshitama, K., Teramoto, S. & Komamine, A. Isolation and purification of tyrosine hydroxylase from callus cultures of *Portulaca grandiflora*. *Plant Cell Physiol.* **42,** 969–975 (2001).
31. Guindon, S. & Gascuel, O. A simple, fast, and accurate algorithm to estimate large phylogenies by maximum likelihood. *Syst. Biol.* **52,** 696–704 (2003).
32. Nuin, P. A. S., Wang, Z. & Tillier, E. R. M. The accuracy of several multiple sequence alignment programs for proteins. *BMC Bioinform.* **7,** 471 (2006).
33. Scott, D. A., Hammond, P. M., Brearley, G. M. & Price, C. P. Identification by high-performance liquid chromatography of tyrosine ammonia-lyase activity in purified fractions of *Phaseolus vulgaris* phenylalanine ammonia-lyase. *J. Chromatogr. B* **573,** 309–312 (1992).
34. Shevchenko, A., Tomas, H., Havli, J., Olsen, J. V. & Mann, M. In-gel digestion for mass spectrometric characterization of proteins and proteomes. *Nature Protocols* **1,** 2856–2860 (2006).
35. Rolando, C., Monties, B. & Lapierre, C. in *Methods in Lignin Chemistry* (eds Lin, S. Y. & Dence, C. W.) 334–340 (Springer, 1992).
36. Broeckling, C. D. *et al.* Metabolic profiling of *Medicago truncatula* cell cultures reveals the effects of biotic and abiotic elicitors on metabolism. *J. Exp. Bot.* **56,** 323–336 (2005).
37. Rohde, A. *et al.* Molecular phenotyping of the pal1 and pal2 mutants of *Arabidopsis thaliana* reveals far-reaching consequences on phenylpropanoid, amino acid, and carbohydrate metabolism. *Plant Cell* **16,** 2749–2771 (2004).
38. Franke, R. *et al.* The *Arabidopsis REF8* gene encodes the 3-hydroxylase of phenylpropanoid metabolism. *Plant J.* **30,** 33–45 (2002).
39. Zuo, Y., Wang, C. & Zhan, J. Separation, characterization, and quantitation of benzoic and phenolic antioxidants in American cranberry fruit by GC–MS. *J. Agricult. Food Chem.* **50,** 3789–3794 (2002).

Acknowledgements

We thank D. Huhman and the Noble Foundation Analytical Chemistry Facility for the analysis of soluble phenolic compounds, Dr X. Wang for assistance with protein purification, and Dr L. Gallego-Giraldo for critical reading of the manuscript. This work was supported by a Barrie Foundation Fellowship (to J.B.), The University of North Texas and the BioEnergy Science Center (Oak Ridge National Laboratory), a US Department of Energy (DOE) Bioenergy Research Center supported by the Office of Biological and Environmental Research in the DOE Office of Science.

Author contributions

R.A.D. and J.B. conceived the study; J.B., J.S.-Y., F.C. and R.A.D. designed the experiments; J.B, J.S.-Y. and D.B. performed experimental work; J.B., J.S.-Y., D.B., B.V., F.C. and R.A.D. discussed and interpreted results; J.B. and R.A.D. wrote the paper.

Additional information

Supplementary information is available online. Reprints and permissions information is available online at www.nature.com/reprints. Correspondence and requests for materials should be addressed to R.A.D.

Competing interests

The authors declare no competing financial interests.